Inelastic Scattering Cross Sections for 20-keV Electrons in Al, Be, and Polystyrene*

N. SWANSON AND C. J. POWELL
National Bureau of Standards, Washington, D. C.
(Received 26 July 1965; revised manuscript received 31 December 1965)

Measurements are reported of the inelastic scattering cross sections associated with the characteristic energy losses of 20-keV electrons transmitted through thin films of Al, Be, and polystyrene. These measurements have been made using two techniques which overcome several sources of systematic error in previous measurements. For materials which have narrow characteristic loss lines (such as Al), it is possible to establish the form of the differential cross section and the generalized oscillator strength for the ≈15-eV Al plasmon energy loss for scattering angles between 0 and 20 mrad, the cutoff angle. The differential cross section has been used in repeated two-dimensional folding calculations to correct the intensity measurements of the multiple plasmon losses at the larger scattering angles where unambiguous intensity measurements could not be made. For materials which have broad characteristic loss peaks, such as polystyrene, it is not possible to establish the variation of generalized oscillator strength $f(q)$ with momentum transfer q. If it can be assumed that $f(q)\approx f(0)$ for small q, a cross section for a given loss can be obtained from an energy-loss spectrum measured at one scattering angle. The cross-section measurement accuracy is improved by a comparison of two energy-loss spectra, that of a standard (such as Al) and that of a material of unknown loss cross section, which have been obtained at zero angle under the same measurement conditions. Cross sections of $(1.5\pm0.4)\times10^{-18}$ cm^2 and $(1.5\pm0.5)\times10^{-18}$ cm^2 have been measured for the excitation of the ≈15-eV and ≈19-eV plasmon energy losses in Al and Be, respectively, using the former measurement technique. These values are in good agreement with the cross sections expected theoretically. The second measurement technique has been used to obtain cross sections of $(2.4\pm0.8)\times10^{-20}$ cm^2 and $(1.0\pm0.2)\times10^{-18}$ cm^2 for the 7-eV and 21-eV energy losses, respectively, in polystyrene. The corresponding oscillator strengths $f(0)$ are in good agreement with those deduced recently by LaVilla and Mendlowitz. Values were also obtained for the Al loss-dispersion constants, $\Delta E(\theta)=14.8+(1.39\pm0.07)\times10^4\theta^2+(1.2\pm0.2)\times10^7\theta^4$ (energy loss ΔE in eV, scattering angle θ in radians), and for the critical wave vector for plasmon excitation $k_c=1.46\pm0.07$ Å^{-1}.

1. INTRODUCTION

WHILE there has been a large number of independent measurements of characteristic energy losses of electrons for a variety of solid materials,[1,2] there have been relatively few measurements of the corresponding cross sections for excitation, either in differential or integral form. It is the purpose of this paper to point out several sources of systematic error in previous attempts to measure total cross sections and to present the results of a more rigorous experimental measurement technique which can be utilized in those materials which have narrow characteristic energy-loss lines. For other materials, a comparison technique will be described by which cross sections can be estimated from a measurement of loss spectra at one electron-scattering angle.

It had been intended originally to measure cross sections for the ≈7- and ≈21-eV energy losses in polystyrene[3] in order to make an independent normalization in the determination of the complex frequency-dependent dielectric constant for this material.[4] On account of the large energy breadth of the 21-eV loss and the degradation of the 7-eV loss intensity under electron bombardment,[3] it was decided that it would be possible to measure the cross sections only from a zero-angle loss spectrum, suitable corrections being made to correct for the fraction of loss intensity not measured. The accuracy of this correction can be appreciably increased if the angular properties of the apparatus can in effect be determined from the zero-angle loss spectrum of some standard material. Aluminum was chosen as a standard material suitable for this purpose, on account of its stability (with a ≈20-Å protective oxide layer), its relatively narrow loss peaks, and because its characteristic loss spectrum is relatively simple and well understood.

The mean free path for the dominant 15-eV plasmon loss in aluminum has been recently measured to be 810±60 Å at a primary electron energy of 20 keV by Marton, Simpson, Fowler, and Swanson[5] (MSFS). This mean free path corresponds to a limited angular integration of the experimental loss intensity. A new measurement of the mean free path for the Al loss is reported in Sec. 4 where intensity contributions over larger scattering angles than those considered by MSFS are included in a final experimental cross section. This cross section can be meaningfully compared with the Bethe[6] and Ferrell[7,8] cross-section formulas, and good agreement has been obtained.

Two methods have been used to improve the accuracy of the experimental Al cross section. Firstly, measure-

* Work partially supported by the Atomic Energy Commission, Division of Biology and Medicine.

[1] L. Marton, L. B. Leder, and H. Mendlowitz, in *Advances in Electronics and Electron Physics*, edited by L. Marton (Academic Press Inc., New York, 1955), Vol. 7, p. 183.
[2] O. Klemperer and J. P. G. Shepherd, Advan. Phys. **12**, 355 (1963); H. Raether, Ergeb. Exakt. Naturw. **38**, 84 (1965).
[3] N. Swanson and C. J. Powell, J. Chem. Phys. **39**, 630 (1963).
[4] R. LaVilla and H. Mendlowitz, J. Phys. **25**, 114 (1964).
[5] L. Marton, J. A. Simpson, H. A. Fowler, and N. Swanson, Phys. Rev. **126**, 182 (1962).
[6] H. Bethe, Ann. Physik **5**, 325 (1930).
[7] R. A. Ferrell, Phys. Rev. **101**, 554 (1956).
[8] R. A. Ferrell, Phys. Rev. **107**, 450 (1957).

ments of the angular intensity distribution of the dispersed plasmon loss out to the cutoff angle have established the form of the differential cross section which is in good agreement with that predicted by Ferrell. Secondly, the plasmon differential cross section has been used in a computer program to derive the angular distributions of intensity of the higher order loss peaks at those relatively large scattering angles where unambiguous intensity measurements cannot be made (on account of the factors discussed in Sec. 3.1). These computed angular distributions were fitted to the experimental angular distributions in the small-angle region where reliable intensity measurements could be made. A mean free path could then be obtained by fitting the areas under the composite curves to a Poisson distribution.

To test the feasibility and accuracy of the comparison technique, an independent measurement was made of the mean free path for the 19-eV loss in beryllium using the same technique as for aluminum. On account of the greater breadth in energy of the Be loss peaks, reliable intensity measurements could only be made at small scattering angles and it was not possible to measure experimentally the form of the differential cross section. As the theoretical and experimental forms of the differential cross section for Al were in satisfactory agreement, it was considered reasonable to assume that the theoretical differential cross section for Be could be used in the angular folding calculations.

Comparisons were then made of the zero-angle Al and Be loss spectra under the same measurement conditions. Within the experimental uncertainties, this experiment gave results consistent with the independent measurements of mean free path in Al and Be, and it was considered possible to obtain useful values of mean free paths for the polystyrene energy losses.

A summary of the relevant theory is given in Sec. 2. The criteria to be satisfied for valid cross-section measurements are discussed in Sec. 3.1 and the shortcomings of previous experiments are described in Sec. 3.2. The apparatus used in the present work is described briefly in Sec. 3.3. The measurements of cross section for the dominant losses in Al and Be are presented in Sec. 4 and discussed in relation to previous work. The comparison technique is described in Sec. 5, and the measurements of the cross sections for the two polystyrene losses are described. Finally, in Sec. 6, the angular variations in the Al characteristic loss spectra are analyzed to derive the dispersion constants and the critical wave vector for plasmon excitation.

2. THEORY

Characteristic energy losses, generally of about 5 to 25 eV, occur by excitation of valence or more weakly bound core electrons through a single-electron transition or a collective or plasmon excitation. Theory for the former type of interaction has been developed by Bethe[6] while theory for the latter has been presented by Bohm and Pines,[9] and subsequent workers.[7,8,10] The Bethe theory has been generalized by Fano[11] to include any type of longitudinal excitation, and a general theory of the electron-medium interaction in terms of the macroscopic medium properties has been developed by several authors.[1,11–13] A recent review of the current theoretical situation is given by Fano.[14]

The differential cross section for an optically allowed single-electron transition in a free atom involving a change in energy $\Delta E_{0n}=\hbar\omega_{0n}$ (a transition from state 0 to state n) and a change in momentum q of the primary exciting electron is

$$d\sigma_{0n}=\frac{4\pi e^4}{mv^2}\frac{f_{0n}(q)}{\hbar\omega_{0n}}\frac{dq}{q}, \tag{1}$$

where e and m are the electronic charge and mass, and v is the velocity of the primary electron.[6,11,15] Using the dipole approximation, the generalized oscillator strength $f_{0n}(q)$ can be expressed in terms of the dipole moment matrix element x_{0n} in the limit $q\rightarrow 0$ by $f_{0n}(0)=2m\omega_{0n}|x_{0n}|^2/\hbar$; that is, the oscillator strengths for excitations by photons or electrons are identical in the limit $q\rightarrow 0$. It is usually assumed[15] that $f_{0n}(q)=f_{0n}(0)$ for $q<q_m$, where

$$q_m=(2m\Delta E_{0n})^{1/2}. \tag{2}$$

Recent measurements of $f_{0n}(q)$ by Lassettre and collaborators[16] for various allowed atomic transitions, however, have shown variations in $f_{0n}(q)$ (by a factor ≈ 2) for $q<q_m$. The behavior of $f_{0n}(q)$ for $q>q_m$ depends on the characteristics of the particular transition.[11,17]

The differential cross section for inelastic electron scattering due to plasmon excitation[18] can be expressed in the form[8,11,14]

$$d\sigma_p=\frac{4\pi e^4}{mv^2}\frac{f_p(q)}{\hbar\omega_p}\frac{dq}{q}, \tag{3}$$

where $\Delta E_p=\hbar\omega_p$ is the excitation energy; for a free-electron gas, $\omega_p=(4\pi ne^2/m)^{1/2}$, where n is the electron

[9] D. Bohm and D. Pines, Phys. Rev. **82**, 625 (1951); D. Pines and D. Bohm, *ibid.* **85**, 338 (1952); D. Bohm and D. Pines, *ibid.* **92**, 609 (1953); D. Pines, *ibid.* **92**, 626 (1953).

[10] P. Nozières and D. Pines, Phys. Rev. **109**, 741 (1958); **109**, 762 (1958); **109**, 1062 (1958); **111**, 442 (1958); **113**, 1254 (1959).

[11] U. Fano, Phys. Rev. **103**, 1202 (1956); **118**, 451 (1960).

[12] J. Hubbard, Proc. Phys. Soc. (London) **A68**, 976 (1955).

[13] H. Frohlich and H. Pelzer, Proc. Phys. Soc. (London) **A68**, 529 (1955).

[14] U. Fano, Ann. Rev. Nucl. Sci. **13**, 1 (1963).

[15] H. S. W. Massey, in *Advances in Electronics and Electron Physics*, edited by L. Marton (Academic Press Inc., New York, 1952), Vol. 4, p. 1.

[16] For example, E. N. Lassettre and E. A. Jones, J. Chem. Phys. **40**, 1222 (1964); E. N. Lassettre and M. E. Krasnow, *ibid.* **40**, 1248 (1964); E. N. Lassettre and S. M. Silverman, *ibid.* **40**, 1256, (1964); S. M. Silverman and E. N. Lassettre, *ibid.* **40**, 1265 (1964).

[17] S. M. Silverman, Phys. Rev. **111**, 1114 (1958).

[18] While a differential inverse mean free path would be a more physically meaningful parameter for a collective process, it is convenient to use here an equivalent cross section.

density. The oscillator strength $f_p(q)$ represents the fraction of electrons participating in the excitation.

It has been shown[7,8,10] that plasmon excitations are well defined only for momentum transfer $q<q_c$, where

$$q_c=\hbar k_c=\beta\hbar k_0, \tag{4}$$

where k_c is the critical wave vector for plasmon excitation and k_0 is the wave vector of an electron at the Fermi surface (assumed spherical).

Using a free-electron model to describe the valence electrons, the parameter β has been determined by Nozières and Pines[19] to be

$$\beta=0.47r_s^{1/2}, \tag{5}$$

and by Ferrell[8] and Sawada *et al.*[20] in the form

$$r_s=6.02\beta^2[(2+\beta)\ln(1+2/\beta)-2]^{-1}, \tag{6}$$

where $r_s=(3/4\pi na_0^3)^{1/3}$ and $a_0=\hbar^2/me^2$.

Ferrell[8] has found the plasmon oscillator strength $f_p(q)$ to be

$$f_p(q)=\omega(q)G^{-1}(q)/\omega_p, \tag{7}$$

where $\omega(q)$ is given by the plasmon dispersion relation[8,21,22]

$$\frac{\omega(q)}{\omega_p}=1+\beta^2\left(\frac{6}{5}\gamma^2-\frac{3}{40}\right)\left(\frac{q}{q_c}\right)^2+\beta^4\left(\frac{\gamma^2}{2}-\frac{6\gamma^4}{35}\right)\left(\frac{q}{q_c}\right)^4+\cdots \tag{8}$$

and γ, the ratio of the Fermi energy E_0 to the plasmon energy, is equal to $\hbar k_0^2/2m\omega_p$. The function $G^{-1}(q)$ provides a smooth cutoff for the plasmon differential cross section; $G^{-1}(0)=1$ and $G^{-1}(q_c)=0$. This function has been computed by Ferrell in two regions of q, $q\approx 0$ and $q\approx q_c$, and the behavior of $G^{-1}(q)$ for intermediate q has been obtained by interpolation.

Ferrell[8] has also shown that to order $(q/q_0)^2$, $f_p(q)=1$. That is, within the above free-electron approximation, the plasmon contribution to the stopping power for small momentum transfer is the maximum permitted by the sum rule ($f_p+\sum_n f_{0n}=1$). For q approaching q_c, the plasmon contribution to the stopping power is reduced, and the continuum of single-electron excitations becomes more prominent. One would then expect that Eq. (3) could be used to predict the differential scattering cross section for those materials in which a single[23] characteristic loss was observed and identified on the basis of optical or other evidence as being due to plasmon excitation. Specifically, Ehrenreich, Philipp, and Segall[24] have shown that the oscillator strengths for single-electron excitations of the valence electrons in aluminum are small.

It has been found that collective effects should occur quite generally in condensed matter.[8,11,14,19,25] For some materials, for example, the transition and noble metals, an energy loss due to plasmon excitation may be well defined and be observed in addition to one or more energy losses due to single-electron excitation. In such materials, it would be expected that $f_p(0)<1$ and that Eq. (1) could be applied to the single-electron excitations with values of $f_{0n}(q)$ appropriate to the particular transitions. The distinction between collective and single-electron excitations is less well defined in ionic and molecular solids. For such materials, Eqs. (1) and (3) could be used for the observed energy losses and with the corresponding experimentally determined values of $f(q)$.

The total cross section for a single-electron excitation for $q<q_m$ can now be found by integrating Eq. (1).

$$\sigma_{0n}=\frac{4\pi e^4}{mv^2}\frac{1}{\hbar\omega_{0n}}\int_{q_{\min}}^{q_m}\frac{f_{0n}(q)dq}{q} \tag{9}$$

$$\approx\frac{4\pi e^4 f_{0n}(0)}{mv^2\hbar\omega_{0n}}\ln[2(E/\Delta E_{0n})^{1/2}], \tag{10}$$

where $q_{\min}=\Delta E_{0n}/v$. Similarly, the total cross section for plasmon excitation can be found by integrating Eq. (3), using Eq. (7),

$$\sigma_p=\frac{4\pi e^4}{mv^2}\frac{1}{\hbar\omega_p{}^2}\int_{q_{\min}}^{q_c}\frac{\omega(q)G^{-1}(q)dq}{q}, \tag{11}$$

where $q_{\min}=\Delta E_p/v$.

A polynomial expression for $G^{-1}(q)$ has been obtained[26] by a least-squares fit to values of $G^{-1}(q)$ computed for aluminum and beryllium, and is

$$G^{-1}(u)=1.00-0.3886u+3.158u^2-11.512u^3+15.829u^4-8.069u^5, \tag{12}$$

where $u=q/q_c$. The accuracy of fit of Eq. (12) for both aluminum and beryllium was about 2% over most of the range of u except for the region close to $u=1$ where $G^{-1}(u)$ varies rapidly and the error was as high as 10%. This latter error is not significant as the differential cross section is relatively small near $u=1$.

Using Eqs. (8) and (12), with β given by Eq. (6), Eq. (11) was numerically integrated using constants applicable to aluminum and the resulting cross section found to be about 4% less than if it had been assumed that

$$\omega(q)G^{-1}(q)/\omega_p=1 \quad \text{for} \quad q_{\min}\leq q\leq q_c.$$

[19] P. Nozières and D. Pines, Phys. Rev. **113**, 1254 (1959).
[20] K. Sawada, K. A. Brueckner, N. Fukuda, and R. Brout, Phys. Rev. **108**, 507 (1957).
[21] V. P. Silin, Zh. Eksperim. i Teor. Fiz. **37**, 273 (1959) [English transl.: Soviet Phys.—JETP **10**, 192 (1960)].
[22] P. Nozières and D. Pines, Phys. Rev. **111**, 442 (1958).
[23] We exclude from consideration here the surface plasmon loss which is observed with small probability using thick (≈1000 Å) films in transmission experiments. For a summary of those metals for which no energy losses due to single-electron transitions are detected see J. L. Robins, Proc. Phys. Soc. (London) **79**, 119 (1962).
[24] H. Ehrenreich, H. R. Philipp, and B. Segall, Phys. Rev. **132**, 1918 (1963).
[25] D. Pines, Rev. Mod. Phys. **28**, 184 (1956).
[26] Using Eqs. (47), (49), and (51) of Ref. 8.

In those materials where the above free-electron theory can be applied ($f_p(0)\approx 1$), Eq. (11) can be simplified to become

$$\sigma_p \approx \frac{4\pi e^4}{1.04 m v^2 \hbar\omega_p} \ln(\hbar k_c v/\Delta E_p). \quad (13)$$

In materials where the free-electron theory cannot be applied,

$$\sigma_p \approx \frac{4\pi e^4 f_p(0)}{m v^2 \hbar\omega_p} \ln\left(\frac{\hbar k_c v}{\Delta E_p}\right). \quad (14)$$

While β and k_0 are now not well-defined, the value of k_c in Eq. (14) does not have to be known precisely as it affects σ_p logarithmically. It is noted that the upper limits q_m and q_c in the above integrations are both of similar magnitude for excitations ΔE_{0n} and ΔE_p of comparable value. Using Eqs. (2), (4), and (5), $q_m/q_c = 1.09(\Delta E_{0n})^{1/2}/(\Delta E_p)^{1/3}$, where the excitation energies are expressed in eV.

Equation (1) has been derived specifically for electron scattering by atoms. No modifications to the theory have been presented in the case of electron scattering by solids, though it would be expected[14,15,27] that Eq. (1) could be used with changes in the ΔE_{0n} and $f_{0n}(q)$ from those characteristic of the corresponding free atoms. Also, quite apart from any change in the functional form of the $f(q)$, the oscillator strengths for electron and photon excitations in solids are no longer identical when $q \to 0$.[11,19,24]

It is convenient to discuss the experimental work in terms of the electron-scattering angle θ. For small θ, this variable is related to the momentum transfer q by the relation[7,11] $q = P(\theta^2+\theta_E^2)^{1/2}$, where $\theta_E = \Delta E/2E$, and E and P represent the energy and momentum, respectively, of the primary electron.

3. EXPERIMENTAL METHOD

3.1 Criteria for Cross-Section Measurements

Several experimental methods[5,28–33] have been used previously to integrate through various angular ranges the intensities of inelastically scattered electrons and so obtain mean free paths in various materials. The necessity of making a correct angular integration has been recently emphasized and discussed by MSFS.

Following Wentzel[34] and Ferrell,[7] MSFS have expressed the probability $J_N(\theta;t)$ that an electron has been scattered into an element of solid angle at angle θ (here understood to have a vector significance) after traveling a path length t in a specimen foil and after having experienced N inelastic scattering processes of the same type in the form

$$J_N(\theta;t) = D_N(t)\Theta_N(\theta),$$

where

$$D_N(t) = t^N e^{-t/\lambda}/N!$$

and

$$\Theta_N(\theta) = \int\int d^2\theta_{N-1} \int\int d^2\theta_{N-2} \cdots \int\int d^2\theta_1 \times \int\int d^2\theta_0 \Theta_0(\theta_0) F(\theta_0,\theta_1)\cdots F(\theta_{N-1},\theta). \quad (15)$$

In Eq. (15), the double integrals represent two-dimensional convolutions, $\Theta_0(\theta_0)$ represents the angular distribution of the unscattered beam which is assumed to be symmetrical about the $\theta=0$ axis, $F(\theta_{N-1},\theta_N)$ represents the inelastic differential cross section for scattering between θ_{N-1} and θ_N, and λ is the mean free path for the scattering process. It can then be shown that

$$\int\int_{|\theta|=0}^{\theta_{\max}(N)} J_N(\theta;t)d^2\theta = P_N(t/\lambda) = (t/\lambda)^N e^{-t/\lambda}/N!. \quad (16)$$

For $N=0$, the choice of the limit of integration $\theta_{\max}(0)$ is given by the angular extent of the primary beam. For $N\geq 1$, the choice of $\theta_{\max}(N)$ is important, and depends on the type of inelastic process, as discussed in Sec. 2. Suitable values for $\theta_{\max}(N)$ are $N\theta_m+\theta_{\max}(0)$ for energy losses due to single-electron excitation or $N\theta_c+\theta_{\max}(0)$ for energy losses due to plasmon excitation, where $\theta_m = q_m/P$ and $\theta_c = q_c/P$.

Except for MSFS, who determined $P_N(t/\lambda)$ and hence t/λ using $\theta_{\max}(1)\approx\frac{1}{3}\theta_c$, no previous workers have attempted to determine correctly values of $P_N(t/\lambda)$ as indicated by the double integration of Eq. (16). In practice, it is necessary to ensure that $\Theta_0(\theta_0)$, the solid angle of acceptance of the energy analyzer, and the range of scattering angles $\theta_{\max}(N)$ for which intensity contributions are measured are all such that meaningful values of $P_N(t/\lambda)$ are obtained.

It is also necessary to ensure that two spurious sources of electron intensity are avoided in the experimental integration of loss intensity [Eq. (16)]. As indicated in Fig. 1, there is firstly an intensity contribution from electrons scattered inelastically through small angles (arising from the peak in the differential cross section [Eqs. (1) and (3)] near $\theta=0$) and elastically through large angles; in Fig. 1 it can be seen that this "undispersed" peak of electrons resulting from a double-scattering process has reached an intensity greater than the fully dispersed peak of singly scattered electrons for scattering angles greater than about 13 mrad (at an electron energy of 20 keV). Secondly, there is an intensity contribution from the background continuum which is important for angles greater than about 10 mrad. Again, no previous workers except MSFS

[27] C. B. Wilson, Proc. Phys. Soc. (London) **76**, 481 (1960).
[28] G. Ruthemann, Ann. Physik **6**, 113 (1948).
[29] W. Lang, Optik **3**, 233 (1948).
[30] A. W. Blackstock, R. H. Ritchie, and R. D. Birkhoff, Phys. Rev. **100**, 1078 (1955).
[31] G. W. Jull, Proc. Phys. Soc. (London) **B69**, 1237 (1956).
[32] H. J. Watson, Ph.D. thesis, University of Florida, 1962 (unpublished).
[33] C. Kunz, Z. Physik **167**, 53 (1962).
[34] G. Wentzel, Ann. Physik **69**, 335 (1922).

have specifically avoided these unwanted intensity contributions in their determinations of $P_N(t/\lambda)$; Kunz[33] and others, however, have obtained values of $P_N(t/\lambda)$ from spectra recorded when $\theta > \theta_c$.

3.2 Review of Previous Experiments

Some early estimates of mean free path were derived from the characteristic loss spectra obtained by Ruthemann[28] and Lang.[29] It is not possible, however, to determine the nature of the angular integration by which these published spectra were obtained.

An extensive series of measurements of mean free paths was reported by Blackstock *et al.*[30] who used a primary electron beam of unspecified angular width and an analyzer of 30-mrad angular acceptance. By recording the energy-loss spectrum of electrons scattered within the angular limits of their detector, these authors compared the relative intensities of the no-loss peak and the various multiples of the plasmon peaks to deduce values of t/λ. Blackstock *et al.* obtained mean free paths for the dominant losses in aluminum, magnesium, and copper, values being obtained for aluminum as a function of primary energy in the range 25 to 100 keV.

Jull[31] has reported a value of the mean free path of 10-keV electrons in aluminum using a "finely-collimated" primary beam and an analyzer of acceptance 5 mrad. The aluminum loss peaks in this work appear on a large inelastic background, presumably due to the substrate.

Watson[32] has derived values for the mean free path of 15–40-keV electrons in Al and other elements. There is no information in this report on the angular characteristics of the primary beam and of the detector, nor of whether or not a continuum level has been subtracted before determining peak areas. It is therefore very surprising that Watson obtains mean-free-path data consistent with Eq. (13) over a relatively large primary energy range. Neither the measurements of Blackstock *et al.*, Jull, or of Watson could have eliminated the intensity contributions of double elastic-inelastic scattering or of the background continuum referred to in Sec. 3.1, and it is also unlikely that the intensities of each loss multiple were weighted properly for any single primary electron energy in the angular integration [Eq. (16)]. Furthermore, the dependence of the upper limit in the integration of Eq. (16) on primary electron momentum requires that the analyzer angular acceptance be modified when cross-section measurements are made over a wide energy range.

MSFS determined a mean free path for aluminum at 20 keV by two methods. Firstly, they integrated the loss intensities from $\theta=0$ to $\theta=6$ mrad under conditions of good angular resolution. By truncating the intensity of the first loss at 6 mrad for several specimens, and comparing the integrated loss intensity with the integrated no-loss intensity, they obtained t/λ from two-point fits to Eq. (16) and hence values for λ representative of the scattering to 6 mrad. Secondly, in an experiment with a relatively wide (≈ 2 mrad) primary beam, they compared loss peak areas from a spectrum recorded at zero angle and were able to obtain an 8-point fit to a Poisson distribution from which they derived a value of λ representative of scattering from $\theta=0$ to about $\theta=2$ mrad.

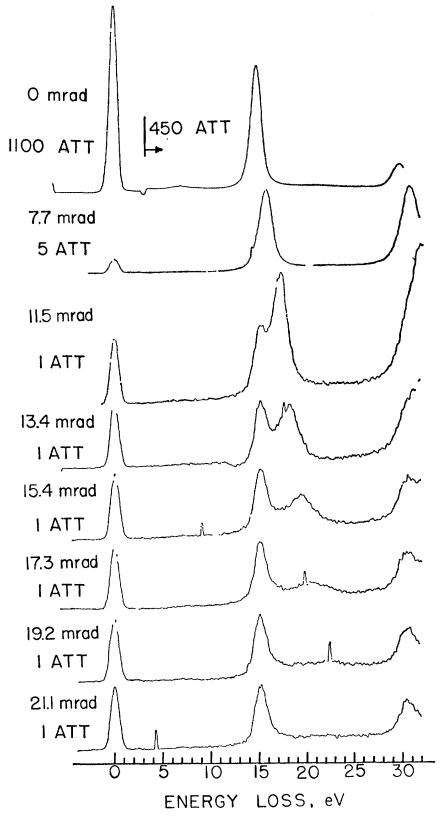

FIG. 1. Recorder traces of characteristic loss spectra obtained with a 1000-Å aluminum specimen for the various electron-scattering angles and intensity attenuation ratios indicated. The occasional spikes in some spectra are noise pulses due to electrical discharges in the detector system.

A third method of determining mean free paths has been described by Kunz.[33] Using an apparatus of high angular resolution, he compared the intensity of the no-loss peak at a scattering angle a little greater than the plasmon cutoff angle in aluminum with the intensity at the same angle of the "undispersed" peak of electrons that had been inelastically scattered within a cone of half-angle $\approx\theta_c$ and also elastically scattered to appear at the angle of measurement. It is implicitly assumed in this type of measurement that the differential cross section for elastic scattering (out to $\theta\approx\theta_c$) of the cone of inelastically scattered electrons is approximately constant over most of the cone. That this is not the case can be seen from the work of Boersch *et al.*[35] A more

[35] H. Boersch, H. Miessner, and W. Raith, Z. Physik **168**, 404 (1962).

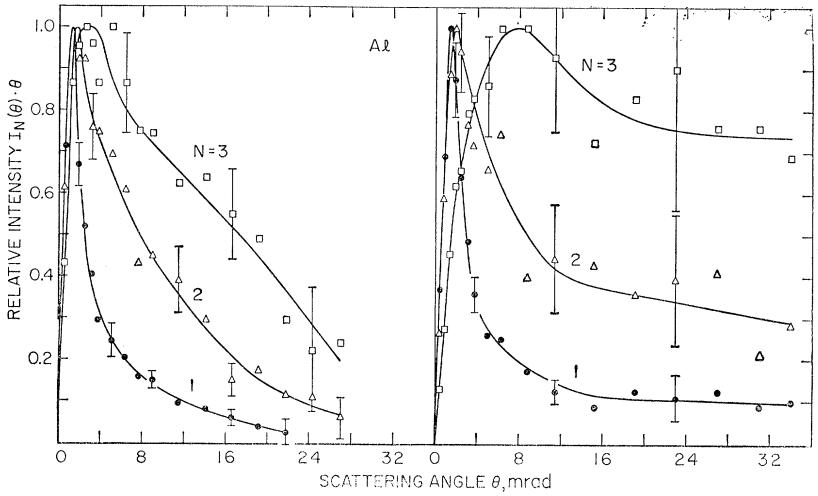

FIG. 2. First moments $I_N(\theta)\cdot\theta$ of the measured intensity $I_N(\theta)$ as a function of electron-scattering angle θ for the Nth loss multiple in an 880-Å aluminum specimen and a 1420-Å beryllium specimen. Each curve has been normalized so that the maximum in $I_N(\theta)\cdot\theta$ is unity. The vertical error bars represent the estimated errors in the peak areas due to the uncertainty in the continuum level and the reproducibility of the data. For Be, the dispersed and undispersed loss peaks could not be separated, and the experimental points represent the combined intensity.

accurate measurement of mean free path might be obtained if the various peak areas at some scattering angles several times θ_c were compared, though in practice the measurement would not be very accurate due to the relatively low signal current at these angles and to the uncertainty in the continuum level.

3.3 Apparatus

Electron energy-loss spectra were obtained at a primary energy of 20 keV, using an energy analyzer with resolution of about 1 eV.[5] The primary beam has an angular distribution which is approximately Gaussian, with a typical full angular width at half-maximum of 1.6 mrad. The angular acceptance of the analyzer is $\approx$0.25 mrad. The scattering angle can be varied by rotating the gun and specimen jointly with respect to the analyzer. The intensity of the scattered electrons is recorded as a function of energy loss for a given scattering angle, using a phosphor-photomultiplier combination operated as a linear detector.

4. INDEPENDENT MEASUREMENTS OF λ FOR Al AND Be

4.1 Specimen Preparation

The Al and Be films were prepared by vacuum evaporation onto a Victawet 35B substrate at a pressure $\approx 10^{-5}$ Torr. These films were floated off the substrate on water and mounted over the 0.5-mm-diam aperture of the specimen holder. The film thicknesses were measured by the Tolansky multiple-beam interferometer technique[36] using specimens picked up on glass microscope slides and coated with an evaporated silver layer. The measured thicknesses for two sets of specimens of each element were 1990 and 880 Å for Al and 2220 and 1420 Å for Be. Two successive measurements on the same specimen edge agreed to 1%, and values for a given specimen were consistent to within 2% for Al and 5% for Be.

Some Al specimens were picked up on Al-coated slides for the thickness measurement, in principle eliminating the error due to different sticking coefficients for the evaporated silver across the specimen edge. The Al-backed films had larger measured thicknesses than the glass-backed films by varying amounts of up to several hundred angstroms. This result is in agreement with the experience of MSFS, and the opposite of the result obtained by Aisenberg[37] for some other metals. Two Al evaporations were made later using a quartz crystal microbalance to measure the mass thickness. The values given by the microbalance were generally within 100 Å of the thickness measurements obtained on a glass substrate using the bulk density. The thickness values for glass-backed Al specimens were therefore taken to be correct within $\pm$100 Å. The Be specimen thicknesses were not checked this way, and an uncertainty of $\pm$150 Å was assigned to these measured thicknesses. A. R. Wolter [J. Appl. Phys. **36**, 2377 (1965)] has recently reported that thin Al films had bulk density (within the experimental accuracy of about 5%) in the thickness range 200 to 5000 Å. T. E. Hartman [J. Vac. Sci. Tech. **2**, 239 (1965)], however, finds the density of Al films of thickness less than 500 Å to be up to about 25% less than the bulk density, while films in the 600- to 2000-Å thickness range had densities of about 3% less than the bulk value. As the variation of film thickness would be expected to depend on the film preparation conditions, the assigned errors in thickness are considered reasonable estimates; the quartz crystal microbalance was not available until after the present films had been prepared and used.

[36] S. Tolansky, *Surface Microtopography* (Interscience Publishers, Inc., New York, 1960).

[37] S. Aisenberg, in *Transactions of the Tenth National Vacuum Symposium 1963* (The MacMillan Company, New York, 1963), p. 457.

4.2 Method

The energy-loss spectra were recorded as a function of electron scattering angle for the specimen films of aluminum and beryllium. Typical loss spectra obtained from a 1000-Å aluminum specimen are shown in Fig. 1. These spectra are similar although not identical to those published by Kunz.[33]

From the measured angular distribution of intensity $I_N(\theta)$ of each loss multiple N, plots were made of the relative number of electrons $\theta I_N(\theta)$ of each loss scattered through the angle θ. Typical plots of the first moments of the measured intensities for Al and Be are shown in Fig. 2.

For scattering angles smaller than about 10 mrad, the measurement of the loss peak areas is relatively straightforward, but for larger angles some assumptions have to be made regarding the loss-peak line shape and the level of the continuum background. At zero angle, the loss-peak line shape has been established as being close to the Lorentzian line shape that would be expected from a free-electron model.[38] Measurements have been made of the increase in width of the plasmon loss peak in Al with increasing scattering angle; the magnitude of the change in width and its comparison with the relevant theory is discussed in a separate paper.[39] At the larger angles, the dispersed Al loss peak still appears symmetrical, but it is not possible to determine unambiguously the relative intensity distributions of the continuum, the dispersed loss peak, and of the tails from the neighboring peaks at $\approx$15-eV and $\approx$30-eV energy loss.

MSFS determined peak areas in Al after subtracting an assumed continuum level obtained by drawing a line through the troughs between the peaks. This is certainly an overestimate of the continuum intensity, particularly in the region of the higher order loss peaks of larger breadth where the intensity contribution between peaks from overlapping tails would be relatively greater than in the vicinity of the first loss peak. In the present work, an attempt was made to estimate a "reasonable" level of the continuum consistent with the assumption that there was a discrete loss-peak intensity above the continuum associated with overlapping Lorentzian tails. The uncertainty in the location of the continuum for beryllium is greater than for aluminum on account of the broader beryllium loss peaks and the consequent greater overlapping.[38] The small intensity of the surface plasmon loss often observed below the first bulk plasmon loss has not been included with the bulk plasmon loss intensity.

Glick and Ferrell[40] have predicted the change in the continuum with scattering angle, but it has not been possible to confirm these predictions on account of the peaks of electrons inelastically scattered near zero angle and elastically scattered through angles greater than $\approx$10 mrad. It was also considered unwise to use these predictions to estimate the continuum intensity distribution without solving the problem of deriving the changes in the predicted continuum distribution due to multiple inelastic scattering in the relatively thick films used in this work.

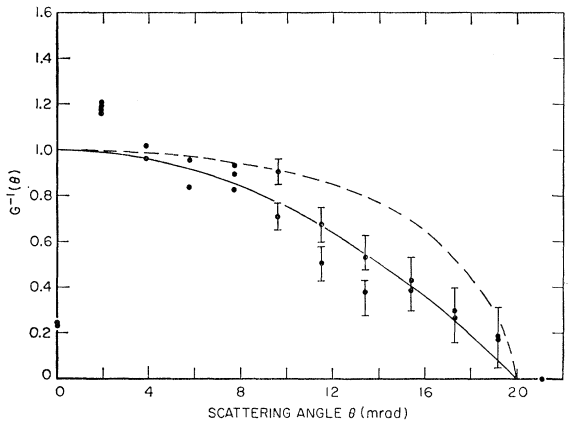

FIG. 3. The solid circles are measured values of $I_1(\theta)\times(\theta^2+\theta_E^2)/\Delta E(\theta)$ as a function of scattering angle θ using loss spectra obtained with a 1000-Å aluminum specimen. $I_1(\theta)$ is the measured intensity of the first plasmon loss [energy loss $\Delta E(\theta)$] and the error bars represent the uncertainty in locating the continuum (Fig. 1). No angular unfolding of the data was performed to compare the experimental data with the Ferrell $G^{-1}(\theta)$ curve (dashed line). The solid curve shows $G^{-1}(\theta)=1-(\theta/\theta_c)^2$, a function that was also used in the folding computations ($\theta_c=20$ mrad).

From Eqs. (3) and (7), it would be expected that

$$d\sigma_p \propto \omega(\theta)G^{-1}(\theta)d\Omega/(\theta^2+\theta_E^2).$$

Using the measured angular intensity distribution of the first plasmon loss in aluminum, a plot was made of $I_1(\theta)\times(\theta^2+\theta_E^2)/\Delta E(\theta)$ versus θ. This is shown in Fig. 3, and compared with the $G^{-1}(\theta)$ distribution estimated by Ferrell.[26] No correction was made to the experimental curve to account for the finite angular resolution of the apparatus. This was because the form of the differential cross section had been verified by MSFS for small θ ($\omega/\omega_p\approx 1, G^{-1}(\theta)\approx 1$), and it was decided to make the comparison for large θ where the instrumental resolution would not distort the angular plots significantly, except close to $\theta=\theta_c$ if the Ferrell theory was obeyed. Within the limits of the uncertainty associated with the continuum level and shape discussed previously, the experimental curve agrees satisfactorily with that expected from Eq. (12). The differences between experiment and the Ferrell theory for θ near θ_c may be real but are not significant in the determination of mean free paths as the differential cross section [Eq. (3)] is relatively small in this region (see Sec. 4.3). The form of the differential cross section found here agrees with previous experimental determinations[33,35,41]; no

[38] N. Swanson, J. Opt. Soc. Am. **54**, 1130 (1964).
[39] B. W. Ninham, C. J. Powell, and N. Swanson (following paper) Phys. Rev. **144**, 209 (1966).
[40] A. J. Glick and R. A. Ferrell, Ann. Phys. (N. Y.) **11**, 359 (1960).
[41] P. Schmüser, Z. Physik **180**, 105 (1964).

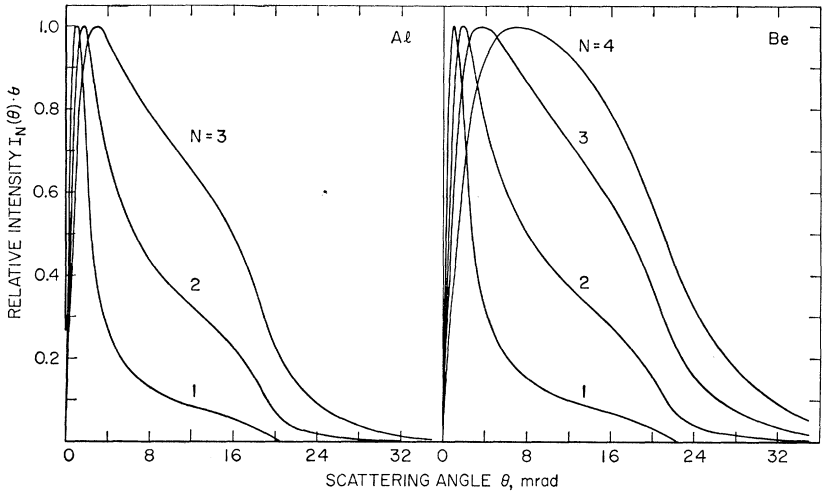

FIG. 4. Computed first moments $I_N(\theta)\cdot\theta$ for aluminum and beryllium as a function of θ. Compare with the experimental data shown in Fig. 2.

attempt was made to search for deficiencies in $d\sigma/d\theta$ for $\theta<1$ mrad of the type found by Schmuser,[41] as such deficiencies, if due to surface effects, would not be significant in the relatively thick films of the present work, and were not detected by MSFS.

To overcome the uncertainties in the measurements of the intensities of the higher order losses at large angles due to low signal current, the determination of the continuum level, and the inability to resolve the fully dispersed and "undispersed" loss components, it was decided to compute the form of the angular distributions of these losses using Eq. (3) and assuming Eqs. (8) and (12) were exact. These computed distributions could be fitted to the experimental curves in the angular region between 0 and 10 mrad where the signal-to-noise ratio was good and the uncertainties associated with the continuum and with elastic scattering were small.

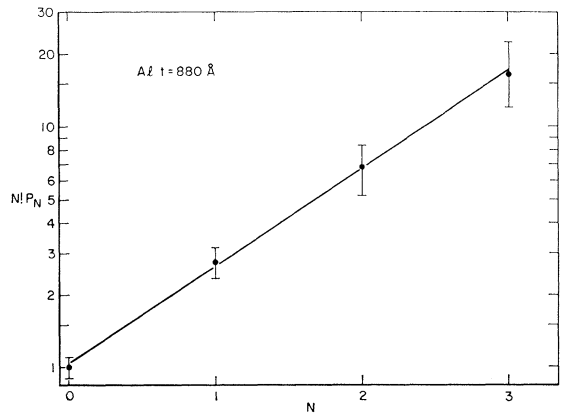

FIG. 5. Plot of $N!P_N$ as a function of N, using data obtained from an 880-Å aluminum specimen. The straight line is the least-squares fit, from which the argument t/λ of the Poisson distribution [Eq. (16)] is derived. The error bars on the points represent the uncertainties in the values of P_N due to the intensity fluctuations in the small-angle region and to the matching of the experimental and computed curves of $I_N(\theta)\cdot\theta$.

A computer program was written in which a two-dimensional folding of an appropriate angular distribution of the primary beam with the differential cross section Eq. (3) was performed. This computed angular distribution of the first plasmon loss was similarly folded with the differential cross section again to generate the angular distribution of the second multiple plasmon loss, and so on, as represented by Eq. (15). Free-electron values of γ were used in Eq. (8), and for aluminum the experimental value of $\theta_c=20$ mrad and a corresponding value of β were used in Eqs. (8) and (12). It was not possible to measure θ_c for beryllium, but on the basis of Eq. (4), the cutoff angle in beryllium would be expected to be about 10% higher than for aluminum. Hence in calculations applicable to beryllium θ_c was arbitrarily set equal to 22 mrad and a corresponding value of β was used.

The computed first moments of each loss for Al and Be are shown in Fig. 4. The most striking feature of these distributions is that most of the intensity of each loss occurs within a cone of semiangle little greater than θ_c; the computed intensities up to $\theta=\theta_{\max}(2)$, $\theta_{\max}(3)$, $\cdots$ for $N=2, 3, \cdots$ are finite but relatively very small. This feature of the curves is due to the $G^{-1}(\theta)$ factor eliminating intensity contributions for scattering angles greater than θ_c. Similar curves to those in Fig. 4 have been obtained by changing the input angular distribution, eliminating the term in the differential cross section due to dispersion, and replacing the function for $G^{-1}(u)$ in Eq. (12) by other polynomials.

The computed curves were fitted to the experimental curves in the 2–8-mrad angular region and the areas under the composite curves ($=P_N(t/\lambda)$) were measured for each N. Using the same procedure as MSFS, the argument t/λ in the Poisson distribution Eq. (16) was obtained from the slope of a least-squares straight-line fit of $\log(N!P_N)$ against N with each point weighted inversely to its estimated error, as indicated in Fig. 5. In this figure, the error bars associated with each point

were estimated from the uncertainties in the measurement of the P_N and due to the finite drifts in signal current and in alignment during the course of the angular sweep. The latter source of error was minimized by recording loss spectra for scattering angles both above and below the plane of the analyzer and averaging the areas. The maximum error in t/λ is estimated to be 15% for Al and 20% for Be.

4.3 Results

A summary of the measurements of t, t/λ, and λ is shown in Table I for each specimen. The mean experimental values of mean free path for each element λ_e, and the corresponding cross sections σ_e (computed assuming the films had bulk density) are shown in Table II with the theoretical cross sections σ_t predicted by Eq. (13). Within the experimental uncertainties, there is good agreement between the corresponding values of σ_e and σ_t.

It can be seen from Fig. 5 that the points for $N \geq 2$ lie within the experimental uncertainty on the straight line obtained using the points at $N=0$ and $N=1$ alone, for which no appreciable systematic error is introduced by the method of fitting computed angular distributions to obtain the relative intensities of the higher order losses. This last factor together with the assumption of cylindrical symmetry in the primary beam constitute the main sources of known possible systematic error in the results. In beryllium, there were additional sources of systematic error due to the inability to resolve adequately the various loss peaks leading to uncertainties in the form of the differential cross section and the cutoff angle θ_c (Fig. 2).

Due to the approximations involved in deriving the form of $G^{-1}(\theta)$,[8] it was considered desirable to see how the computed angular distributions depended on $G^{-1}(\theta)$. From Fig. 3, it would seem that a reasonable fit to the experimental points is given by

$$G^{-1}(u)=1-u^2. \tag{17}$$

A computation was made of the angular intensity distributions for the Al losses using Eqs. (3), (8), and (17). Fitting these distributions to the small-angle region of the experimental curves and following the same analysis procedure as before, a mean value for the aluminum mean free path was found to be 380 Å which is only 20 Å higher than the value of λ_e obtained previously using Eq. (12). It is concluded that the systematic error due to not knowing the precise form of $G^{-1}(u)$ is smaller than the other errors associated with the present experimental methods.

No correction for specimen oxidation has been made to the measured film thicknesses. Over periods of the order of a year, the energy-loss spectra were found to be reproducible and to show no measurable inelastic intensity that could be attributed to surface oxides or other contaminants. As the effective metal thicknesses would be smaller than the measured thicknesses, the measured mean free paths might be too large by up to about 20 Å. This latter source of systematic error is of the opposite sign and of comparable magnitude to that associated with the possible systematic error in the form of $G^{-1}(u)$. It is therefore considered that no further correction should be applied to the values of λ_e.

TABLE I. Summary of measurements of mean free path for aluminum and beryllium. The errors in film thickness were assigned as discussed in Sec. 4.1 of the text and the quoted errors in t/λ were obtained from the probable errors associated with the least-squares fits (Fig. 5). The final error in λ includes in addition an estimate of the systematic errors as discussed in the text and in the caption to Fig. 2.

Element	Specimen thickness t(Å)	Number of points in fit	t/λ	Mean free path λ(Å)
Al	880±100	4	2.56±0.02	345±90
Al	880±100	3	2.07±0.01	425±125
Al	1990±100	4	6.43±0.06	310±80
Be	1420±150	4	4.92±0.11	290±90
Be	1420±150	5	5.17±0.17	275±85
Be	2220±150	4	9.18±0.56	240±65

4.4 Discussion

It is believed that the necessary criteria described in Sec. 3.1 for valid cross-section measurements for electron energy losses in solids have been satisfied for the first time in the present work. The close agreement between the values of σ_e and σ_t for both Al and Be indicates that $f_p(0)\approx 1$. This is to be expected, on the basis of the sum rule,[14] as no significant amount of inelastic intensity is detected other than the plasmon loss and its multiples in each metal.

The present results are also consistent with the results of Ehrenreich *et al.*[23] who found $f_p(0)=2.6/3.0=0.87$ for Al by an analysis of optical data and of LaVilla and Mendlowitz[42] who found $f_p(0)=0.92$ for Be by an analysis of zero-angle characteristic loss spectra. Because $f_p(0)$ is so close to unity, it is considered that the use of the free-electron formulas for $f_p(q)$ in Sec. 4.2 is justified.

While no previous measurements have been made of the mean free path for the 19-eV Be loss, several measurements have been made of the mean free path for the 15-eV loss in Al. Though these latter measurements cannot be directly compared with the present results,

TABLE II. Values for aluminum and beryllium of the average experimental mean free paths λ_e, the corresponding cross sections σ_e, and the theoretical cross sections σ_t predicted using Eq. (13).

	Al	Be
λ_e(Å)	360±90	270±80
σ_e(cm^2)	$(1.54\pm0.38)\times10^{-18}$	$(1.51\pm0.45)\times10^{-18}$
σ_t(cm^2)	1.73×10^{-18}	1.30×10^{-18}

[42] R. LaVilla and H. Mendlowitz, Appl. Opt. 4, 955 (1965).

for the reasons discussed in Secs. 3.1 and 3.2, most of these results nevertheless agree at least qualitatively with the λ_e found here.

Blackstock *et al.*[30] report a value of mean free path in Al of about 625 Å for an electron energy of 25 keV, while Jull[31] obtains 260 Å for 10-keV electrons, and Watson[32] obtains 370 Å for 20-keV electrons. These numerical values can be compared with the present result for 20-keV electrons using Eq. (13). It would seem likely that the above authors have obtained qualitatively reasonable values of mean free path because of two factors. Firstly, it would appear that in the work of Blackstock *et al.*, at least, the experimental integration was made over an angular range which in some cases was comparable to θ_c. In such cases, one would expect reasonable agreement between experimental and theoretical mean free paths (Sec. 4.2). The second factor is associated with the assumption made by Kunz[33] that of those electrons elastically scattered a certain fraction will be inelastically scattered, as given by Eq. (16) with the same argument t/λ as for the main inelastic scattering of interest. This will be true as long as it can be assumed that all inelastic scattering between $\theta=0$ and $\theta=\theta_c$ is both included in the intensity measurement and correctly weighted. While neither of these latter two assumptions is valid, the errors introduced into the Poisson fits may be small.

Kunz[33] quotes a value for the Al mean free path of 750 Å ±40% for 39-keV electrons. He estimates that there is a 20% uncertainty in his film thickness and a further 20% uncertainty in continuum estimation. Horstmann and Meyer[43] have used the same technique as Kunz to obtain a mean free path of 1000 Å for 51-keV electrons in Al, with similar uncertainties. There is a further uncertainty in both results on account of the factors discussed in the previous paragraph. An estimate of the uncertainty in using Kunz's method was obtained by comparing the areas under the no-loss and first and second plasmon loss peaks of the $\theta=23$-mrad spectrum shown in Fig. 1. One finds from this comparison that $t/\lambda=1.70$ and hence $\lambda=580$ Å. While there are uncertainties in the continuum location of the order of 20% and in the film thickness of about 10%, this value of mean free path is about 60% higher than the λ_e found here.

MSFS obtained values of mean free path equal to 810±60 Å for Al in an experiment where the angular integration was over a range from $\theta=0$ to $\theta\approx2$ mrad and 820±220 Å in an experiment where the integration range was from $\theta=0$ to $\theta=6$ mrad.[44] Both results are consistent with the present result, within the experimental uncertainties of each measurement, though no attempt has been made to estimate any error in the former result on account of the varying portion of each loss intensity occurring between $\theta=0$ and $\theta\approx2$ mrad, compared with the total loss intensity over all allowed angles (cf. Fig. 4).

The main concern of this paper has been to make meaningful comparisons between theory and experiment of differential [Eq. (3)] and total [Eq. 13)] inelastic scattering cross sections for Al and Be. The variation of cross section with primary electron energy constitutes a separate experimental problem which could not be undertaken without redesigning the present apparatus. Previous measurements of mean free path as a function of electron energy have been reported by Blackstock *et al.*,[30] Watson,[32] and by Brunger and Menz.[45]

5. DETERMINATION OF λ FROM ZERO-ANGLE LOSS SPECTRA: APPLICATION TO POLYSTYRENE

5.1 Method

It is apparent from the discussion in Secs. 3.1 and 3.2 that a mean free path can only be rigorously determined in an apparatus of good angular resolution (≈1 mrad at 20 keV) where the loss peak concerned is sufficiently narrow to separate "undispersed" and fully dispersed loss components and where some reasonable estimate can be made of the level of the background continuum. Unfortunately, few materials have sufficiently narrow loss peaks to enable the corresponding mean free paths to be measured unambiguously as described.

In materials such as polystyrene, it is not possible to measure reliably angular distributions of loss intensity and so establish a differential cross section. A method will be described by which a value of a mean free path for a given loss can be obtained if the functional form of the oscillator strengths $f(q)$ in Eqs. (1) and (3) is known. For losses due to plasmon excitation, Eq. (7) could be used to estimate $f_p(q)$, though for broad plasmon loss peaks the use of the free-electron expressions for $G^{-1}(q)$ and $\omega(q)$ would be doubtful and it is preferred here to assume $f_p(q)=f_p(0)$ for $q<q_c$. For losses due to single-electron excitation, the form of $f_{0n}(q)$ is not generally known and, to obtain a cross section, it is necessary to assume[15,16] that $f_{0n}(q)=f_{0n}(0)$ for $q<q_m$. With these assumptions, a mean free path can be deduced from a measurement of a characteristic loss spectrum at one scattering angle, correction being made for that fraction of the angular distribution not measured using the differential cross-section formulas, Eqs. (1) and (3). It would be desirable to make this measurement at zero-scattering angle on account of the optimum signal and it would also be desirable to retain good angular resolution to eliminate dispersion effects and any intensity contribution away from zero angle arising from elastic scattering or continuum

[43] M. Horstmann and G. Meyer, Z. Physik **182**, 380 (1965).

[44] Three values of t/λ quoted by MSFS using two-point fits each have an uncertainty of about ±10%. Dr. H. A. Fowler (private communication).

[45] W. Brunger and W. Menz, Z. Physik **184**, 271 (1965).

inelastic scattering. The areas under the loss peaks of spectra observed at zero angle must be multiplied by an angular weighting factor F which, under conditions where the primary electron beam has negligibly small angular width, would be defined by

$$F=\left[\int_0^{\theta_{\max}}(d\sigma/d\theta)d\theta\right]\Big/H, \tag{18}$$

where

$$H=\int_0^{\theta_1}\frac{d\sigma}{d\theta}d\theta \tag{19}$$

and where θ_1 is the semiangle of acceptance of the energy analyzer. In the present experiment, the angular width of the primary beam was greater than both θ_E and θ_1 and was well approximated by a Gaussian of parameter θ_0

$$\phi(\theta)=\exp(-\theta^2/2\theta_0^2)/(2\pi)^{1/2}\theta_0. \tag{20}$$

Values of H were computed by a two-dimensional folding of Eq. (20) with the differential cross section given by Eq. (1) [with $f(q)=f(0)$] and using representative values of θ_0, θ_1, and θ_E.

While it would be possible to derive a mean free path from zero-angle spectra of a given material, using the ratio of the appropriate value of F to a factor E which takes account of the fraction of the no-loss intensity not measured, useful results could be obtained in practice only if the instrumental angular characteristics were known to a relatively high degree of precision. Less precise knowledge is required of the instrumental characteristics if a comparison can be made of the loss spectra at zero angle of two materials A and B under the same conditions of observation.[46]

If the ratio of the intensity of a given loss peak to that of the no-loss peak (at zero angle) in material A is I_{A1}/I_{A0} and the corresponding ratio for material B is I_{B1}/I_{B0}, then the value of $(t/\lambda)_B$ can be expressed in terms of $(t/\lambda)_A$ by

$$\left(\frac{t}{\lambda}\right)_B=\frac{I_{A0}E_A}{I_{A1}F_A}\frac{I_{B1}F_B}{I_{B0}E_B}\left(\frac{t}{\lambda}\right)_A. \tag{21}$$

It has been implicitly assumed in this and previous work that when the primary electron energy is much larger than the energy loss under consideration, the no-loss and the various orders of loss-electrons suffer essentially the same attenuation due to elastic or other types of inelastic processes. It would therefore appear reasonable to assume that $E_A/E_B=1$ when the spectra of two materials are compared under the same conditions. This assumption also implies that there is no appreciable modification of the form of the angular distribution of the primary beam on transmission through either specimen. In the present series of comparisons, no significant difference was found in the angular distribution of the no-loss beam on transmission through either of a pair of specimens, and it was possible to follow the procedure described below. If θ_0 had been different for the two specimens, it would have been necessary to compute appropriate values of E and F for each material.

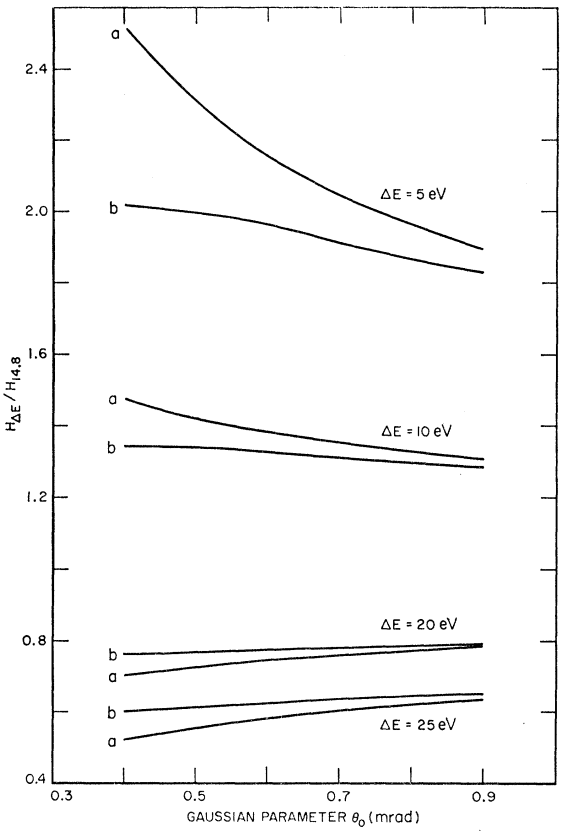

FIG. 6. The ratios $\Delta E H_{\Delta E}/14.8H_{14.8}$ as a function of the Gaussian parameter θ_0 describing the primary-beam angular distribution [Eq. (20)] for $\Delta E=5$, 10, 20, and 25 eV and for analyzer acceptance semiangles of 0.25 mrad [curves (a)] and 1.0 mrad [curves (b)]. Note: The ordinate is incorrectly labeled.

For the reasons described in the Introduction, aluminum was chosen as a standard material. To estimate the uncertainties in cross-section measurements for representative values of θ_E, values of H were computed for energy losses of 5, 10, 14.8, 20, and 25 eV and the ratios $\Delta E H_{\Delta E}/14.8H_{14.8}$ are shown in Fig. 6 for various instrumental conditions (ΔE for Al=14.8 eV). In this work θ_0 was generally between 0.7 and 0.9 mrad, and θ_1 was taken to be 0.25 mrad.[5] The uncertainty in the ratio $H_{\Delta E}/H_{14.8}$ is typically less than 5% and is much smaller than the uncertainties in the other quantities appearing in Eq. (21).

In the comparisons reported below, an 880-Å aluminum film was used for reference. Using the value of $\lambda_e=360$ Å, a value of $(t/\lambda)_{Al}=2.44\pm0.37$ was adopted in applying Eq. (21).

A specimen holder was used in this phase of the work on which the Al reference film was mounted at 90°

[46] Kindly suggested to us by Dr. J. Arol Simpson.

TABLE III. Average values of the mean free paths for the 7- and 21-eV energy losses in polystyrene obtained by comparisons of polystyrene and aluminum loss spectra at zero angle. These values are representative of electron scattering out to limiting angles (θ_{max}) of 19 and 22 mrad for the 7- and 21-eV losses, respectively.

Film thickness (Å)	Mean free path for 7-eV loss (Å)	Mean free path for 21-eV loss (Å)
1200±200	22 200±7000	505±140
1620±140	12 600±3500	365±90

to the other specimen film. Successive loss spectra could then be taken merely by rotating the specimen holder and recentering in the primary beam.

5.2 Comparison of Zero-Angle Spectra of Al and Be

In order to examine the validity of the above comparison technique and to ensure that there were no significant sources of unknown systematic error, comparisons were made of the zero-angle spectra of Al and Be. The mean free path for Be could then be checked against that reported in Sec. 4.3.

In applying Eq. (21), values of F_{Al} and F_{Be} were calculated from Eq. (18) with the numerator obtained from Eq. (13) and the denominator obtained by separate calculations of H applicable to Al and Be. The results of two separate zero-angle comparison runs where Al and Be loss spectra were recorded in succession gave $\lambda_{Be}=280$ Å and 300 Å, with a probable error of ±70 Å, which compare favorably with the value of $\lambda_e=270$ ±80 Å for Be shown in Table II.

5.3 Comparison of Zero-Angle Spectra of Al and Polystyrene

In view of the above satisfactory derivation of the Be mean free path by comparison of zero-angle spectra, it was decided to obtain mean free paths for the energy losses in polystyrene in a similar way. Polystyrene was chosen for investigation as there was interest in its optical properties in the vacuum ultraviolet region.[4]

Polystyrene films were prepared from a 1% by weight solution of atactic polystyrene in benzene.[3] Specimen film thicknesses measured for specimens picked up on both clean glass slides and polystyrene coated slides gave results which overlapped; the differences were believed to arise more from actual variations in specimen thickness than from different substrates. Two sets of polystyrene specimens, with thicknesses of 1200±200 Å and 1620±140 Å, were used; the stated errors include the measurements using both substrates.

The polystyrene loss spectrum shows a narrow peak at 7 eV and a broader, more intense peak at 21.3 eV. It proved more difficult to obtain reliable intensity data on the 7-eV loss than on the 21-eV loss, because of rapid deterioration of the 7-eV loss with exposure to the beam.[3] Nevertheless, an attempt was made to measure the angular characteristics of the 7-eV loss between 0 and 20 mrad. Within the uncertainties due to change in loss position and intensity with electron bombardment as well as to the factors discussed in Sec. 3, it was not possible to observe a dispersion of the 7-eV loss, any change in the form of the differential cross section caused by a possible $f(q)$ factor, or any evidence of a cutoff angle. The large width of the 21-eV peak precluded any useful analysis of its angular characteristics.

In measuring the areas of the peaks in the zero-angle spectrum, the 7-eV loss peak was considered to lie on the sloping tail of the 21-eV peak. The 21-eV peak was assumed to be symmetrical about the peak maximum and include all the area under the loss, i.e., no continuum background was assumed. The loss peak was in fact symmetrical out to an amplitude of about 50% of its peak amplitude, and at least part of the asymmetry beyond this point was due to the presence of the second multiple of the 21-eV loss.

LaVilla and Mendlowitz[4] have concluded that the 21-eV loss in polystyrene is due principally to a collective excitation. The 7-eV loss is associated with a single-electron excitation but it is believed that the loss intensity is enhanced by collective effects, the real part of the complex dielectric constant departing significantly from unity.

In the calculation of the appropriate F factors using Eq. (18), values of H were computed for each polystyrene loss and θ_{max} was chosen to be 19 mrad for the 7-eV loss [Eq. (2)] and 22 mrad for the 21-eV loss [Eqs. (4) and (5)]. It should be noted that the F values are not particularly sensitive to the choice of θ_{max}.

The results of the mean-free-path determinations are shown in Table III. The quoted errors are probable errors estimated from the uncertainties in film thickness, in the measurement of loss-peak areas, and in the value used for t/λ for aluminum. While there is reasonable agreement in the values from the two specimens for the mean free path of the 21-eV loss, there is a large difference between the two values for the 7-eV loss, barely within the limits of uncertainty of each measure-

TABLE IV. Mean values for the 7- and 21-eV energy losses in polystyrene of the experimental mean free paths λ_e, the corresponding cross sections σ_e, and the theoretical cross sections σ_t found using Eqs. (10) and (14) (for the 7- and 21-eV losses, respectively). The quantity $f(0)$ is an approximate (see text) measure of the oscillator strength for zero momentum transfer and $Nf(0)$ represents the oscillator strength in terms of the number of electrons of the monomeric unit participating in the excitation ($N=40$).

	7-eV loss	21-eV loss
λ_e(Å)	17 400±5 500	410±80
σ_e(cm²)	$(2.4\pm0.8)\times10^{-20}$	$(1.0\pm0.2)\times10^{-18}$
σ_t(cm²)	$4.62\times10^{-18}f(0)$	$1.21\times10^{-18}f(0)$
$f(0)$	$(5.1\pm1.6)\times10^{-3}$	0.83±0.16
$Nf(0)$	0.20±0.06	33±7

ment. This difference is believed due partly to changes in the 7-eV loss under electron bombardment and thus reflects an uncorrected source of systematic error in the mean-free-path values for the 7-eV loss.

A measurement was made of the angular distribution of the 21-eV loss in the 1620-Å polystyrene specimen. The measured distribution at small angles was extrapolated using a distribution computed with free-electron parameters as described in Sec. 4.2, again with $\theta_{max}=22$ mrad, and a mean free path of 370±70 Å was obtained. The average value of the mean free path for the 21-eV loss is then found to be 410±80 Å.

The average mean free paths λ_e and the corresponding cross sections σ_e are shown in Table IV with the approximate cross sections σ_t calculated using Eq. (10) for the 7-eV loss and Eq. (14) for the 21-eV loss.[47] From the ratio σ_e/σ_t for each loss, an estimate may be made of the oscillator strengths $f(0)$ and $Nf(0)$ for each loss, where $N=40$ is the number of valence electrons in the monomeric unit of the polystyrene structure. It is seen from Table IV that the excitation of the 21-eV loss accounts for almost all the interaction at zero scattering angle determined by the sum rule.[14] LaVilla and Mendlowitz[4] find the oscillator strength ($Nf(0)$) for the 21-eV loss to be 25 to 30 electrons per monomeric unit, in good agreement with the result obtained here. Their value of $Nf(0)$ for the 7-eV loss was about one-half electron per monomeric unit which is about twice the present result. This numerical discrepancy can be attributed to the fact that LaVilla and Mendlowitz did not perform an angular unfolding of the "zero-angle" spectrum; that is, the measured 7-eV loss intensity was a larger fraction of the total 7-eV loss intensity compared to the fraction of the 21-eV loss intensity measured in the zero-angle spectrum.

The oscillator strength for optical absorption in benzene and many of its derivatives for the $A_{1g}\rightarrow E_{1u}$ transition has been previously measured to be 0.7 to 1 electron per molecular unit.[48] It is not surprising that the oscillator strengths for optical and electron excitation are different, even for a solid polymer, as LaVilla and Mendlowitz[4] have shown that the real part of the complex dielectric constant of polystyrene departs appreciably from unity in the 7-eV region.

6. DISPERSION PARAMETERS AND THE CUTOFF ANGLE IN ALUMINUM

It is of interest to derive from the spectra in Fig. 1 the parameters which describe the variation of the Al plasmon energy loss with scattering angle and also the values of the plasmon cutoff angle and the parameter k_c [Eq. (4)]. These quantities have been measured

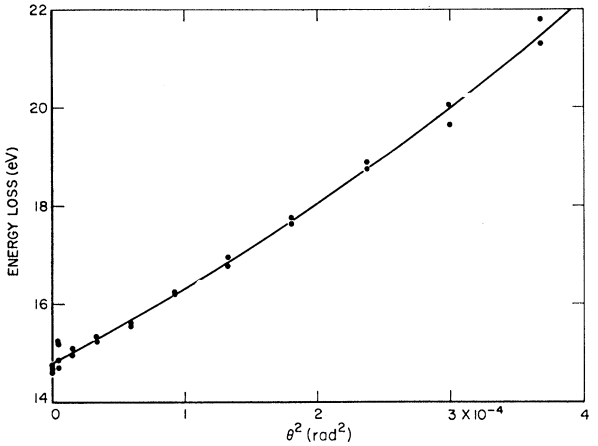

FIG. 7. A plot of the dispersed energy loss $\Delta E(\theta)$ in aluminum (1000-Å specimen) as a function of the square of the scattering angle θ. The points are the individual measurements and the solid curve represents the quadratic least-squares fit: $\Delta E(\theta)=14.8+(1.39\pm0.07)\times10^{4}\theta^{2}+(1.2\pm0.2)\times10^{7}\theta^{4}$.

previously,[33,35,41,49,50] but there is some disagreement in the published data.

Other authors have expressed the dispersion equation (8) in the form

$$\frac{\hbar\omega-\hbar\omega_p}{2E}=\frac{1}{2\gamma}\left(\frac{6\gamma^2}{5}-\frac{3}{40}\right)\theta^2+\frac{E}{2\gamma E_0}\left(\frac{\gamma^2}{2}-\frac{6\gamma^4}{35}\right)\theta^4 =A\theta^2+B\theta^4. \tag{22}$$

The present values of the Al plasmon energy loss as a function of scattering angle are shown in Fig. 7. Most of the uncertainty in the energy-loss values arises from the uncertainty in the location and shape of the continuum at the larger scattering angles. The data in Fig. 7 were fitted by least squares to the equation

$$\frac{\Delta E(\theta)-\Delta E(0)}{2E}=a\theta^2+b\theta^4. \tag{23}$$

Values of a and b are shown in Table V and compared with the previous experimental values and with values of A and B computed using free-electron values of γ and E_0. The constant B is a function of the primary energy used in each experiment, while A is independent of energy.

Neither Meyer[50] nor Kunz[33] reported values of a from their experiments. Values of a and b have been derived from least-squares fits of data points read from their figures showing energy loss versus scattering angle. In Meyer's figure, the point at zero angle (which should be the most accurate) deviates appreciably from the curve expected using the remaining points. An additional least-squares fit was therefore made excluding the zero-angle point. Schmüser[41] has quoted values of a for

[47] It was assumed that the polystyrene film density was 1.05 g cm^{-3}, the bulk density.

[48] H. B. Klevens and J. R. Platt, J. Chem. Phys. **17**, 470 (1949); J. R. Platt, *ibid.* **19**, 101 (1951); H. B. Klevens, J. Polymer Sci. **10**, 97 (1953).

[49] H. Watanabe, J. Phys. Soc. Japan **11**, 112 (1956).

[50] G. Meyer, Z. Physik **148**, 61 (1957).

TABLE V. Comparison of measured and theoretical values of dispersion constants in aluminum [see Eqs. (22) and (23)]. The theoretical value A is independent of primary electron energy while the value B is a function of the primary energy. The parameters a and b represent the corresponding experimental values of the dispersion constants deduced from the work of the author indicated.

Author	Reference number	A	a	B	b
Watanabe	49	0.39	0.50±0.05	3.2×10^2	$(3\pm1)\times10^2$
Meyer: present fit using all points	50		0.53±0.07	3.9×10^2	$-(1.5\pm0.5)\times10^3$
present fit excluding zero-angle point	50		0.37±0.09		$-(5\pm5)\times10^2$
Schmüser's fit	41		0.35±0.06		
Kunz: present fit	33		0.36±0.03	5.0×10^2	$(1.3\pm1.3)\times10^2$
Schmüser's fit	41		0.41±0.02		
Boersch *et al.*	35		0.37±0.02	5.8×10^2	
Schmüser	41		0.40±0.01	5.1×10^2	
Present work			0.35±0.02	2.6×10^2	$(2.9\pm0.5)\times10^2$

Meyer's and Kunz's experiments. The differences between the present fit and Schmüser's quoted values are presumably caused by Schmüser's use of the original data values.

Watanabe[49] is the only previous worker to claim to obtain a value of b. There is evidence of a positive value of b in the work of Kunz, but there is little evidence of a θ^4 term in Schmüser's work. It is not possible to determine whether or not Boersch *et al.*[35] find a θ^4 term as these authors do not show data for the angular region near θ_c.

The present values of a and b agree quite well with A and B. It is reasonable to presume that any differences would be caused by departures from free-electron theory due to the lattice core.

It is also possible to derive from Fig. 1 the cutoff angle for plasmon excitation. The dispersed plasmon peak is still distinctly visible at $\theta=19.2$ mrad, but at $\theta=21.1$ mrad and beyond the intensity in the 20–25-eV loss region seems to be mainly due to the overlapping tails of the ≈15-eV and ≈30-eV losses superimposed on the continuum. The plasmon cutoff angle θ_c is therefore believe to be 20±1 mrad, and the critical wave vector for plasmon excitation 1.46±0.07 Å^{-1}. These values are compared with previous determinations in Table VI.

TABLE VI. Values of the observed plasmon cutoff angle θ_c in aluminum and the corresponding critical wave vector for plasmon excitation k_c [Eq. (4)].

Author	Reference number	θ_c	k_c
Watanabe	49	15-18 mrad	1.25-1.48 Å^{-1}
Kunz	33	15-20	1.55–2.06
Boersch *et al.*	35	13.5±1	1.57±0.15
Schmüser	41	15	1.5
Present work		20±1	1.46±0.07

Using the free-electron value of $k_0=1.75$ Å^{-1} and the present value of $k_c=1.46$ Å^{-1}, the constant $\beta=0.83$. From Eq. (5), it is found that $\beta=0.68$, while using Eq. (6), $\beta=0.74$. In a more recent calculation Brouers and Deltour[51] have deduced a value of $\beta=0.820$ for Al and with which they obtain very good agreement between theoretical and experimental determinations of soft x-ray satellite band intensity.

7. CONCLUSION

New measurements are reported for the mean free paths and cross sections of 20-keV electrons in aluminum and beryllium due to excitation of plasmon energy losses. These new values have been obtained by techniques which are free from the systematic errors and limitations of previous work.

A technique is reported for comparing electron energy-loss spectra of two materials at zero scattering angle and for deducing mean free paths for losses in one material if a value of t/λ is known for a loss in the other. This technique has been used to determine the mean free paths, cross sections, and oscillator strengths for the 7- and 21-eV losses in polystyrene. As this technique is comparatively rapid, it would be desirable to apply it to other classes of material for which mean free paths cannot be reliably determined in any other way.

ACKNOWLEDGMENTS

The authors wish to acknowledge stimulating discussions with their colleagues, particularly Dr. J. Arol Simpson, Dr. C. E. Kuyatt, Dr. H. A. Fowler, and Dr. H. Mendlowitz.

[51] F. Brouers and J. Deltour, Phys. Stat. Solidi **7**, 915 (1964); F. Brouers, Phys. Letters **11**, 297 (1964).